RESEARCH ARTICLE

Multiple Training Stage Image Enhancement Enrolled With CCRGAN Pseudo Templates for Large Area Dry Fingerprint Recognition

CHIH-HAN CHENG[1], CHING-TE CHIU[1], CHIA-YU KUAN[1], YU-CHI SU [1], KUAN-HSIEN LIU[2], TSUNG-CHAN LEE [2], JIA-LIN CHEN[2], JIE-YU LUO[2], WEI-CHANG CHUN[2], YAO-REN CHANG[2], AND KUAN-YING HO [2], (Member, IEEE)

[1]Department of Computer Science, National Tsing Hua University, Hsinchu 300044, Taiwan
[2]Novatek Microelectronics Corporation, Hsinchu 302082, Taiwan

Corresponding author: Yu-Chi Su (suyuqi79@gapp.nthu.edu.tw)

ABSTRACT Fingerprint recognition is widely used in daily life. However, the physiological phenomena of human can still fail recognition under dry and low temperature conditions. We present two main approaches for enhancing the accuracy of fingerprint recognition systems in cases of dry fingerprints. The first approach is an image enhancement algorithm with multiple training stages (MTS) for fingerprints at low temperatures, which aims to restore low quality fingerprints to normal quality. The second method is a Cycled Contrastive Ridge Generative Adversarial Network (CCRGAN) learning framework for synthesizing enrolled templates, aimed at improving the accuracy of low-temperature fingerprint matching in authentication systems. For FVC2002 dataset, we have achieved 0.05% for EER on DB1A, which is better than 0.09% for Li et al. (2022) and 0.18% for Wong and Lai (2020) on the MTS algorithm. After adding CCRGAN pseudo low fingerprint, the EER is improved to 0.0009%. As for inference time, our inference time is about 83 times faster than Li et al. (2022) on the FVC2002 DB3B.

INDEX TERMS Convolution, generators, image processing, image enhancement, neural networks.

I. INTRODUCTION

Fingerprint recognition at low temperature is still a problem that needs to be solved because the moisture on the skin of fingers are significantly reduced, which leads to poor quality of scanned fingerprint images. The ridges of the low-temperature fingerprints might be unclear or the black dots may appear on the images. The challenge in restoring the fingerprint lies in the limited and potentially inaccurate information available in the image. Image processing, such as image enhancement or synthetic enrolled templates, can be used to improve the accuracy of dry fingerprint recognition in low-temperature conditions.

Conventional image enhancement methods are utilized in feature-based fingerprint recognition. Reference [4] used a method based on non-stationary directional Fourier domain

The associate editor coordinating the review of this manuscript and approving it for publication was Zhe Jin .

filtering. They first filtered the image and then set a threshold to get the enhanced result. Reference [5] transferred enhanced image to estimate local ridge orientation and frequency on multi-blocks to improve the valley to be clearer and the ridge structures of input fingerprint images. It is a fast algorithm that can achieve high accuracy. However, if they filtered by estimating the orientation of fingerprints, only finite labels can be presented. This limitation leads to lots of incorrect orientation of the ridges in dry fingerprints at the low temperature, which makes the dry fingerprint recognition system be error-prone.

Previous works proved that the fingerprint image enhancement methods based on single stage neural network have good results [2], [6], [7], and [8]. However, these methods can face the same challenges as conventional image enhancement techniques if not appropriately constrained, leading to potentially incorrect ridge orientation in the enhanced fingerprints.

In this paper, we propose two methods to improve the recognition rate of dry fingerprints. One is that try to enhance the fingerprint images by dividing the task into multiple sub-tasks, called Multiple Training Stage (MTS) algorithm. The MTS algorithm consists of two distinct sets, each addressing a specific aspect of the image enhancement problem. Another approach is to predict the dry fingerprint image by using the user's normal temperature fingerprint image. We perform Cycled Contrastive Ridge Generative Adversarial Network (CCRGAN) to simulate low temperature fingerprint. We evaluate our methods on the FVC2002 and FVC2004 datasets and show that they outperform previous methods. The main contributions of our work are as follows:

- We design an image enhancement algorithm called Multiple Training Stage (MTS) with two subtasks for a template-based matching recognition system.
- We generate the confidence map in the first stage, which can guide the enhancement task in the second stage.
- We perform Cycled Contrastive Ridge Generative Adversarial Network (CCRGAN) to generate pseudo dry fingerprints, which can improve the matching rate of recognition system.
- On the FVC2002 dataset, we have achieved 0.05% for EER on DB1A, which is better than 0.09% for [1] and 0.18% for [2] on the MTS algorithm. With CCRGAN pseudo low, the EER is improved to 0.0009%.
- On the FVC2002 DB3 B, our inference time is about 83 times faster than [3].

II. RELATED WORK

A. FEATURE-BASED MATCHING

Fingerprint recognition systems that rely on specific features of fingerprints for identification purposes, such as ridge orientation, singularity points, region line count, region spacing, and minutiae, are known as feature-based fingerprint systems. Chen and Kuo [9] proposed a method that utilizes non-ink fingerprints and tree matching. Bhanu and Tan [10] and Singh et al. [11] demonstrated advancements in fingerprint indexing by utilizing minutiae triplets and both minutiae and pore features. Jaam et al. [12] introduced a fingerprint recognition approach that combined both orientation and minutiae information to enhance the accuracy of the system. Zhao et al. [13] employed the technique of random sample consensus to enhance the accuracy of their fingerprint recognition system, resulting in improved results. Medina-Pérez et al. [14] introduced a new algorithm for fingerprint matching that addressed limitations associated with conventional minutiae-based algorithms. Sudiro et al. [15] proposed a minutiae-based fingerprint recognition system implemented in FPGA-based hardware, which achieved a lower equal error rate (ERR).

B. TEMPLATE-BASED MATCHING

The templated-based matching system for fingerprint first chooses templates to enroll, which is used to find the matching fingerprint. These techniques have been demon-strated to achieve either better classification accuracy or prevention of attacks on the matching process. Ryu et al. [16] proposed a template adaptation algorithm that utilizes Bayesian estimation to generate a local fingerprint quality information updated minutiae. Cappelli et al. [17] utilized a masquerade attack that reconstructed a fingerprint image from templates based on minutiae to test eight state-of-the-arts fingerprint matching algorithms. Le and Tam [18] examined the usage of a standardized fingerprint model to synthesize fingerprint templates. Random Triangle Hashing was proposed by Jin et al. [19]. However, this approach was only appropriate for a limited number of remote users.

C. IMAGE ENHANCEMENT

Feature-based fingerprint identification systems typically rely on conventional image enhancement techniques. These methods have been found to produce superior results compared to standard techniques proposed by Sherlock et al. [4], who used non-stationary directional Fourier domain filtering. Bansal et al. [20] introduced an efficient algorithm for fingerprint image enhancement, which utilized Type-2 fuzzy logic. By improving the clarity of the valley and ridge structures, they were able to achieve higher verification accuracy in their experiments. In [21], the authors presented an unsupervised learning approach that utilized a convolutional deep network to enhance fingerprint structures for low and high level. Their method outperformed Gabor-based enhancement and short time Fourier transform-assisted enhancement techniques on the FVC2000 database, achieving an EER of 7.4%.

D. SINGLE STAGE NETWORK

Previous research has focused on single-stage fingerprint image enhancement methods, such as [6], [7], [8]. Shen et al. [6] proposed a method using PFE-Net work and Laplacian Loss to enhance fingerprint images with higher resolution. By utilizing the Laplacian Loss, the proposed method sharpened edges and effectively enhanced pore features. However, the technique was only applicable to the reinforcement of unbroken ridges and pores. Li et al. [7] introduced a two-branch Convolutional Neural Network (CNN) consisting of an enhancement branch and an orientation branch to improve the performance. Sivaswamy [8] proposed a network designed for extracting fingerprints from images with a noisy background. Their approach was effective in capturing fingerprints from a variety of backgrounds. However, the processed fingerprints were not exclusively intended for template-based matching.

E. PSEUDO TEMPLATE

Suzuki et al. [22] has shown that using pseudo images can improve the recognition of low-temperature fingerprints. Pseudo images have proven to be effective for matching low-temperature fingerprints in a template-based system. To ensure that the pseudo images are useful for the matching
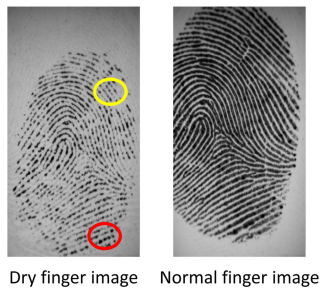
Dry finger image   Normal finger image

FIGURE 1. The low temperature fingerprint image and normal fingerprint image. The whole image is origin pattern. The yellow circle is noise pattern (black dots). The red one is ridge pattern (broken ridge).
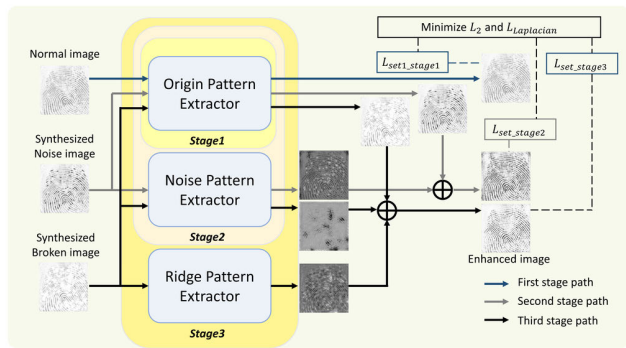

FIGURE 2. The overall architecture of MTS first set.

system, a multi-stage synthesis approach is used instead of a one-time synthesis.

III. MULTIPLE TRAINING STAGE IMAGE ENHANCEMENT

In this section, we introduce the two different sets of our MTS algorithm. Both of sets are used to enhance the low temperature fingerprint images. Due to the characteristics of low temperature fingerprint, direct strengthening will result in irregularities in the fingerprint. Therefore, we divided the task of enhancement into several sub-problems. In the first set, we turn the problem into origin pattern, ridge pattern and noise pattern. In the second set, it is composed of estimating the confidence map and restoring the ridges. We also propose five kinds of training data, which are Normal, Normal Synthesized (NS), Normal Synthesized Version 1 (NSv1), Normal Synthesized Version 2 (NSv2), Normal Confidence (NC) and Normal Local aligned (NL).

A. THE FIRST SET OF MTS

There are three sub-tasks that need to be solved in this set, including the origin pattern, ridge pattern, and noise pattern, as shown in Fig.1. We believe that the low dry fingerprint image problems can be composed of these three sub-tasks. The origin pattern is trained in the first stage, which represents the information in the original images. The ridge pattern is trained in the second stage, which represents the broken ridges in the fingerprint. We observe that there are many discontinuous ridges in low dry fingerprints.

(a)   (b)   (c)   (d)

FIGURE 3. Synthesized data example. (a) Origin Image. (b) NS. (C) NSv1 (d) NSv2.

Reconnecting these ridges can make the style of the low dry fingerprint closer to a normal fingerprint. The noise pattern is trained in the third stage, which represents the black dots in low dry fingerprints. Due to the characteristics of human skin, fingerprints scanned at low temperatures result in irregular black noises on the scanned images. By removing these noises, it can make the enhanced fingerprints closer to normal fingerprints. The overall architecture of the first set for MTS is shown in Fig.2.

1) SYNTHESIZED DATA

We produce three kinds of data, normal synthesized (NS), normal synthesized version 1 (NSv1), and normal synthesized version 2 (NSv2), to simulate the real low temperature fingerprint. NS is the normal data with the black dot. NSv1 is used to simulate the broken ridge. NSv2 is also used to simulate the broken ridge but it is more severe than NSv1 as shown in Fig.3.

2) TRAINING STAGE AND INFERENCE STAGE

The first training stage is focused on the origin pattern. We aim to ensure that the bottleneck features are useful, so the input data and output data are the same. The second training stage focuses on the noise pattern. A new decoder is connected to the bottleneck in this stage, allowing the model to learn how to eliminate the black noise in low temperature fingerprints. The model weights from the first stage are frozen. The third stage is focused on the ridge pattern, where a different decoder is used to solve this sub-task. This decoder is expected to learn how to connect broken ridges. The pretrained weights of the model are frozen in the second stage. During the inference stage, we utilize the entire model to get the enhanced fingerprint.

3) THE SECOND SET MOTIVATION

The synthesized data have a specific pattern, which may limit the performance of the MTS first set. As shown in Fig.4), the block dot noises are removed in the second stage. However, the third training stage makes the noise pattern worse as seen by red circles. So we combine the third stage of ridge connecting and the second stage of noise removing into one stage, known as the ridge restorer in the MTS second set.

B. THE SECOND SET OF MTS

As shown in Fig.5, the process is divided into two stages. The first stage aims to produce a confidence map, and the
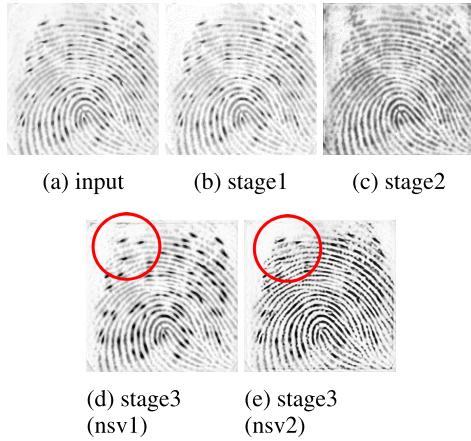
(a) input   (b) stage1   (c) stage2

(d) stage3   (e) stage3
(nsv1)   (nsv2)

FIGURE 4. NS inference on MTS first set.

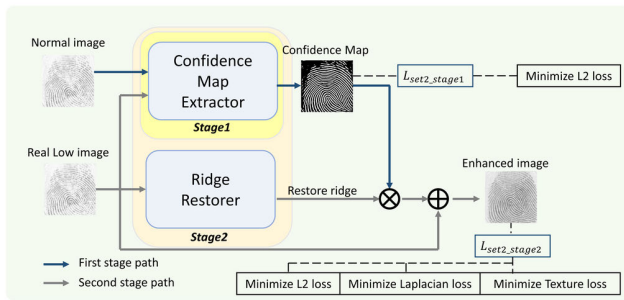**FIGURE 5.** MTS second set overall architecture.
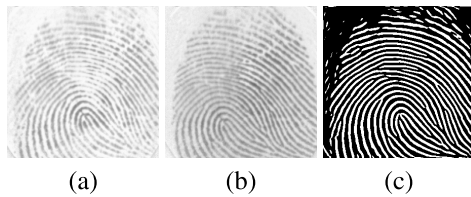

(a)   (b)   (c)

FIGURE 6. The real training data in MTS second set. (a) The low temperature fingerprint data in NL. (b)The normal fingerprint in NL. (c)The confidence map of the real fingerprint (a).

second stage is referred to as the ridge restorer. The first stage estimates the probable region of ridges on the low temperature fingerprint. The higher the pixel value, the higher the likelihood that the area can be enhanced, and vice versa. The ridge restorer, which is trained in stage 2, then restores the ridges based on this confidence map.

1) REAL DATA
We produce two kinds of data, normal low (NL), normal confidence map (NC), to train on our MTS for second set, shown in Fig.6. NC is the confidence map generated from real data. NL is the real low data aligned to real normal data.

2) TRAINING STAGE AND INFERENCE STAGE
In the first training stage, we train the confidence map extractor. It learns how to estimate the ridge contour map.

If the pixel value is close to 1, it is more likely to be a ridge. During the second training stage, the ridge restorer is trained using real low data (NL). It needs to learn how to enhance the low-temperature fingerprint based on the confidence map. The weight of the confidence map extractor is frozen during this stage. During the inference stage, we use the entire network to obtain the enhanced fingerprint. We believe that the low-temperature fingerprint enhancement task can be effectively solved by dividing it into estimating the confidence map and restoring the ridges.

C. LOSS FUNCTION
We use three kinds of loss functions to train MTS, including pixel-wise loss, Laplacian loss [6] and texture loss [23].

1) PIXEL-WISE LOSS
We apply a straightforward objective that optimizes the similarity between the predicted images and ground truth images with L_2 distance [24]. The L_2 distance is based on L_2-norm. Our pixel-wise loss is represented as:

$$L_2(x, y) = \frac{1}{W \times H} \sum_{i=1}^{W \times H} (x_{ij} - y_{ij})^2 \qquad (1)$$

where x is the predicted image and y is the ground truth image. x_{ij} means the ij^{th} pixel in the predicted image and y_{ij} means ij^{th} pixel in the ground truth image.

2) LAPLACIAN LOSS
Laplacian Loss is used to increase the sharpness of the result images [6]. It is represented as:

$$L_{Laplacian} = \sum_{ij} (Lap(x) - Lap(y))_{ij}^2 \qquad (2)$$

where Lap is the convolution with a fix kernel. The value of the kernel is as follow:

$$Lap = \begin{bmatrix} -1 & -1 & -1 \\ -1 & 8 & -1 \\ -1 & -1 & -1 \end{bmatrix} \qquad (3)$$

x is the predicted image and y is the ground truth image.

3) TEXTURE LOSS
In [23], they introduced a new model of natural textures based on the feature spaces of convolution neural networks. It can increase the perceptual quality. The loss is represented as:

$$L_{texture} = \frac{1}{|\Omega_i|} \sum_{uv \in \Omega_i} \left\| e_{uv}^{(i)}(I') - e_{uv}^{(i)}(I) \right\|_2^2 \qquad (4)$$

where I' is the ground truth image $\in \mathbb{R}^{W \times H \times 3}$. I is the predicted image $\in \mathbb{R}^{W \times H \times 3}$. $e^{(i)}(I)$ is the feature $\in \mathbb{R}^{W \times H \times 3}$ produced by the ith layer of VGG19. Ω_i is $[0, \cdot, W_{i-1}] \times [0, \cdot, H_{i-1}]$, which is the spatial domain of $e^{(i)}(I)$. We use $block5\_conv4$ of VGG19 as the features e(the same setting as [23]).

We claim to minimize total loss for first set and second set. For the MTS first set, the total loss L_{set1} for all three stages is as follow:

$$L_{set1} = \lambda_1 \times L_2 + \lambda_2 \times L_{Laplacian} \tag{5}$$

where λ_1 is set as 0.8 and λ_2 is set as 0.2.

For the MTS second set, the total loss L_{set2_stage1} in first training stage is

$$L_{set2\_stage1} = L_2 \tag{6}$$

As for the second stage, the total loss L_{set2_stage2} is

$$L_{set2\_stage2} = \lambda_1 \times L_2 + \lambda_2 \times L_{Laplacian} + \lambda_3 \times L_{texture} \tag{7}$$

where λ_1 is set as 0.8, and λ_2, λ_3 are both set as 0.2.

IV. CCRGAN PSEUDO TEMPLATES
A. OBJECT FORMULATION
The overall flow of CCRGAN is shown in Fig.7. G_N is the generator which produces normal style fingerprints, and G_L is the generator which produces low style fingerprints. D_N and D_L are the discriminators for normal style fingerprints and low style fingerprints respectively. f is the ridge feature extractor. It is used to calculate our Cycled Contrastive Ridge Loss (CCRL). N and L are the normal fingerprint image and low fingerprint image. N_p is the pseudo normal fingerprint represented as $N_p = G_N(L)$. L_c is the cycled low fingerprint represented as $L_c = G_L(N_p) = G_L(G_N)(L)$. The pseudo low fingerprint is represented as $L_p = G_L(N)$, and Cycled normal fingerprint is represented as $N_c = G_N(L_p) = G_N(G_L(N))$.

B. RIDGE FEATURE EXTRACTOR (f)
Cycled Contrastive Ridge Loss function is generated by ridge feature extractor (f). It can make L_p and N_p be closer to the real fingerprint. We believe that the characteristics of the ridges are more effective in determining the quality of the fingerprint. For the architecture of ridge feature extractor, we use the confidence map extractor proposed in III-B and take the second to last layer as our feature maps. The ridge feature extractor is trained like the first stage in MTS second set. For each input image I, we extract its ridge feature I_f by ridge feature extractor f where $f(I) = I_f$.

C. LOSS FUNCTION
1) CYCLED CONTRASTIVE RIDGE LOSS
This loss function claims to make pseudo low not be too low and enhanced low to be normal. For the cycle $N \rightarrow L_p \rightarrow N_c$, we make pseudo low close to real low and away from real normal and cycled normal, and we make cycled normal close to real normal and away from real low and pseudo low. Fig.8 shows the idea. For another cycle, we use same way to calculate the loss function.

Since we think that ridge can be considered as the level of fingerprint quality, we use pretrained confidence map extractor (f) as our ridge feature extractor. For the cycle $N \rightarrow L_p \rightarrow N_c$ and $L \rightarrow N_p \rightarrow L_c$, the Cycled Contrastive

Ridge Loss is represented as (8), as shown at the bottom of the next page, where n, l are the aligned pair from low data L and Normal data N respectively.

2) ADVERSARIAL LOSS
For the generator G_L and its discriminator D_L, we express the objective as:

$$L_{GAN}(G_L, D_L, L, N) = E_{l \sim P_{data}(I_L)}[\log D_L(l)] + E_{n \sim P_{data}(I_N)}[\log(1 - D_L(G_L(N)))] \tag{9}$$

G aims to minimize this objective, and D tries to maximize it [25]. i.e.

$$\min_{G_L} \max_{D_L} L_{GAN}(G_L, D_L, L, N) \tag{10}$$

For the other generator G_N and its discriminator D_N are similar too. i.e.

$$\min_{G_N} \max_{D_N} L_{GAN}(G_N, D_N, N, L) \tag{11}$$

3) CYCLE CONSISTENCY LOSS
The Cycle Consistency Loss is represented as:

$$L_{cyc}(G_L, G_N) = E_{l \sim P_{data}(I_L)}[\|G_L(G_N(l)) - l\|_2^2] + E_{n \sim P_{data}(I_N)}[\|G_N(G_L(n)) - n\|_2^2] \tag{12}$$

which is the same as [25]. To sum up, the total loss L_{CCRGAN} for CCRGAN is represented as:

$$L_{CCRGAN}(G_L, D_L, G_N, D_N) = L_{GAN}(G_L, D_L, L, N) + L_{GAN}(G_N, D_N, N, L) + L_{cyc}(G_L, G_N) + L_{CCR}(G_L, G_N) \tag{13}$$

V. EXPERIMENTAL RESULTS
A. DATASET WORKFLOW
1) NORMAL SYNTHESIZED (NS)
This dataset is used to simulate black noise dots in low temperature fingerprints. To produce these noise dots, we first binarize the image as a ridge label. Then, we add Gaussian noise to the fingerprint ridges, as shown in Fig.9. Each Gaussian noise dot is produced using a Gaussian kernel with different settings, such as kernel size, sigma, darkness, and the probability of noise appearance. We randomly select a pixel on a ridge as the center and then multiply the pixels in a $n \times n$ area around the center with a Gaussian kernel. We adjust the decay parameter so that the noise color on the ridge is lighter than on the valleys.

2) NORMAL SYNTHESIZED VERSION 1 (NSv1)
This dataset is regarded as a ridge pattern and is used to train the first set of MTS. It is designed to simulate broken ridges in low temperature fingerprints. We adjust the settings of the Gaussian noises to make the color lighter rather than darker. This makes the lines in the fingerprint less visible, as shown in Fig.10.
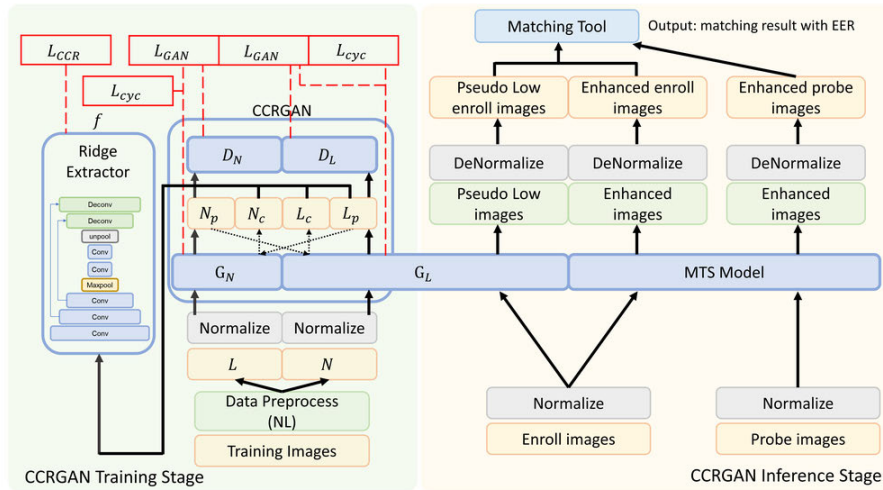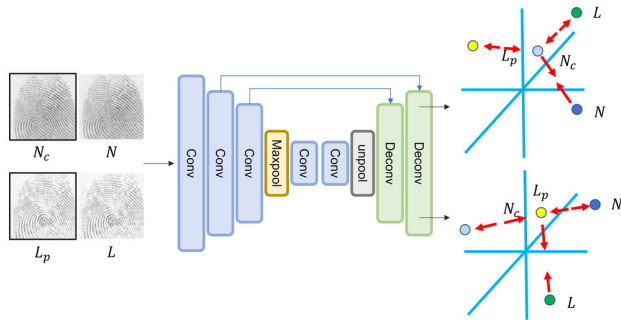
FIGURE 7. Overall flow of CCRGAN.
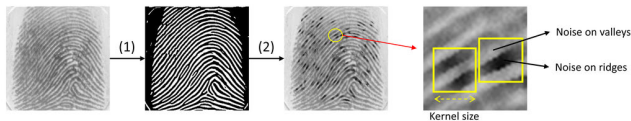

FIGURE 8. The concept of CCRL.

FIGURE 9. The flow of producing NS data.

FIGURE 10. The flow of producing NSv1 data.

FIGURE 11. The flow of producing NSv2 data. The blue circle is Gaussian blur, and the red square is Gaussian noise.

3) NORMAL SYNTHESIZED VERSION 2 (NSv2)

This dataset is regarded as more severe ridge patterns. We add Gaussian blur and Gaussian noise to the image to make the ridges in the area even more obscure, shown in Fig.11.
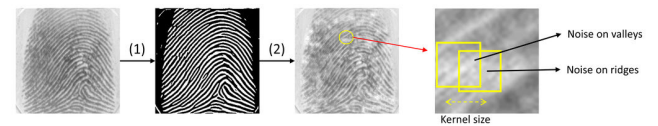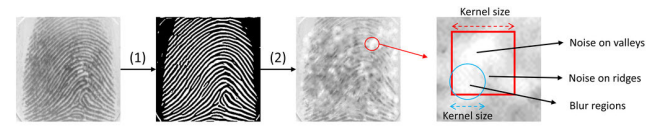
4) NORMAL CONFIDENCE (NC)

To avoid black frames on the pictures, we first flip the picture mirror up and down. Then, we use the method proposed by [5] to generate our confidence map. After getting the result, we crop the center to be our confidence map. The overall flow is shown in Fig.12.

5) NORMAL LOW (NL)

Since our task is to enhance low dry fingerprints, we need pairs of low and normal fingerprints. First, we find the

$$
\begin{aligned}
L_{CCR}(G_L, G_N) = {} & \frac{\| f\,(G_L\,(n)) - f\,(l)\,\|_1}{\| f\,(G_L\,(n)) - f\,(n)\,\|_1 + \| f\,(G_L\,(n)) - f\,(G_N\,(G_L\,(n)))\,\|_1} \\
& + \frac{\| f\,(G_N\,(G_L\,(n))) - f\,(n)\,\|_1}{\| f\,(G_N\,(G_L\,(n))) - f\,(l)\,\|_1 + \| f\,(G_N\,(G_L\,(n))) - f\,(G_L\,(n))\,\|_1} \\
& + \frac{\| f\,(G_N\,(l)) - f\,(n)\,\|_1}{\| f\,(G_N\,(l)) - f\,(l)\,\|_1 + \| f\,(G_N\,(l)) - f\,(G_L\,(G_N\,(l)))\,\|_1} \\
& + \frac{\| f\,(G_L\,(G_N\,(l))) - f\,(l)\,\|_1}{\| f\,(G_L\,(G_N\,(l))) - f\,(n)\,\|_1 + \| f\,(G_L\,(G_N\,(l))) - f\,(G_N\,(l))\,\|_1}
\end{aligned}
\tag{8}
$$

TABLE 1. The training dataset of all methods.

Model	MTS first set			MTS second set		Single Stage	CCRGAN
	1st stage	2nd stage	3rd stage	1st stage	2nd stage	BaseNet[2]	G_L
Data generate from	FVC2000						Private
Training Data-set	Normal	NS	NSv2	NC	NL	NL	NL
Training Patch ♯	100,283	100,283	100,283	100,283	35,356	35,356	11,503
Validating Patch ♯	10,024	10,024	10,024	10,024	3,186	3,186	9,915
Patch size	96×96	96×96	96×96	96×96	72×72	72×72	48×48

FIGURE 12. NC data workflow.

FIGURE 14. The result of overlap count on FVC2002 DB3A. (a) Single Stage [2]. (b)MTS first set.

TABLE 2. FVC2002 DB3A results.

Method	w/o enhance	Single Stage[2]	MTS first set
EER($\downarrow$)	0.006000	0.010000	**0.004000**
FMR50000($\downarrow$)	0.012000	0.026000	**0.012000**
Imposter max score($\downarrow$)	2751	3606	**2324**
FMR50000 score	2308	3057	**2207**
False Reject Count($\downarrow$)	8	20	**6**
Hist Overlap Count($\downarrow$)	7	12	**7**

aligned pairs into patches to be our training data. The overall process is shown in Fig.13.

B. IMPLEMENTATION DETAILS

Our model is trained using TensorFlow on a CPU with a clock speed of 3.9GHz, 132GB of RAM, and an NVIDIA RTX 2080Ti GPU. The batch size and optimizer are set to 32 and Adam with a weight decay of 10^{-5}, respectively. The learning rate is set to 10^{-4}. We use the public FVC2000 dataset for training MTS and private data for training CCRGAN. The results are tested on the FVC2002 and FVC2004 datasets. For the first set of MTS, we use synthesized data because real data cannot be classified into noise pattern and ridge pattern datasets. All MTS models and single stage models are trained on the public dataset. However, CCRGAN is trained on private data because it needs to be trained on the dataset that the dry fingerprint and the normal fingerprint are more different. This is because CCRGAN is used to generate dry fingerprint to add on the matching tool. We want to demonstrate the significant difference in matching results when dry fingerprints are added to the matching tool compared to without the addition of dry fingerprints. The datasets used by all the models are shown in Table 1.

C. ABLATION STUDY

1) EFFECT OF THE MTS AND SINGLE STAGE ON FVC2002 DB3A

To prove that the divide and conquer approach is more effective than solving the task directly, we compare the MTS
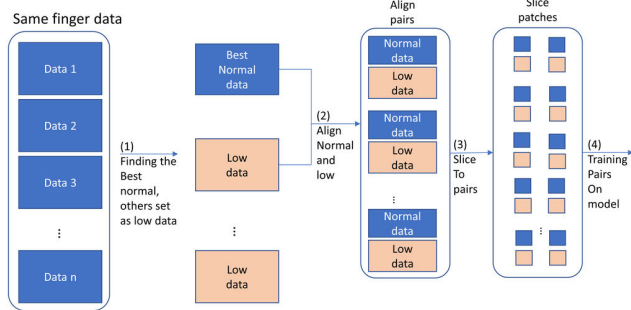

FIGURE 13. The workflow of NL data.

Algorithm 1 Find Best Finger

Input Same finger images I_1 to I_n, and its mask M_1 to M_n
$\forall I \in [0, 255]^{W \times H}$
$\forall M \in [0, 1]^{W \times H}$
$N \leftarrow$ Normalize function from $[min, max] \rightarrow [-1, 1]$
$best \leftarrow None$
$Score_{min} = \infty$

1: **for** $i = 1$ to n **do**
2: $\quad Score_{area} = 1 - \frac{1}{|W \times H|} \sum_{i=1}^{W \times H} M_i$
3: $\quad Score_{quality} = \frac{1}{W \times H} (\sum_{i=1}^{W \times H} (N(M_i) + N(I_i)))^2$
4: $\quad Score_i = Score_{area} + Score_{quality}$
5: $\quad$ **if** $Score_i < Score_{min}$ **then**
6: $\quad\quad Score_{min} = Score_i$
7: $\quad\quad best = I_i$
8: $\quad$ **end if**
9: **end for**
Return best

---

best quality fingerprint among the data of the same finger, as shown in Algorithm 1. This fingerprint is considered the normal fingerprint, while the others are all low fingerprints. Then, we align the normal fingerprint with each low fingerprint using the NovaTek alignment tool to produce many pairs of fingerprints. After alignment, we divide the
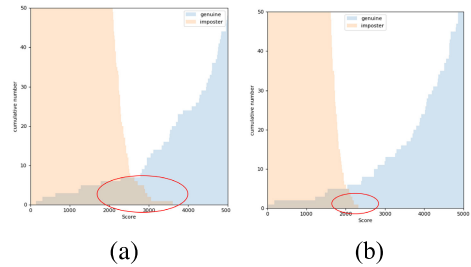
TABLE 3. FVC2004 DB4A results.

Method	w/o enhance	Single Stage[2]	MTS first set	MTS second set	MTS first set+L_p	MTS second set+L_p
EER($\downarrow$)	0.024000	0.016000	0.042000	0.006000	0.020000	**0.004000**
FMR50000($\downarrow$)	0.032832	0.020000	0.114832	0.012000	0.078000	**0.004000**
Imposter max score($\downarrow$)	**1666**	1942	3014	2460	3014	1891
FMR50000 score	1528	1942	2959	1934	2849	1726
False Reject Count($\downarrow$)	20	23	59	10	44	**3**
Hist Overlap Count($\downarrow$)	18	23	57	6	41	**3**
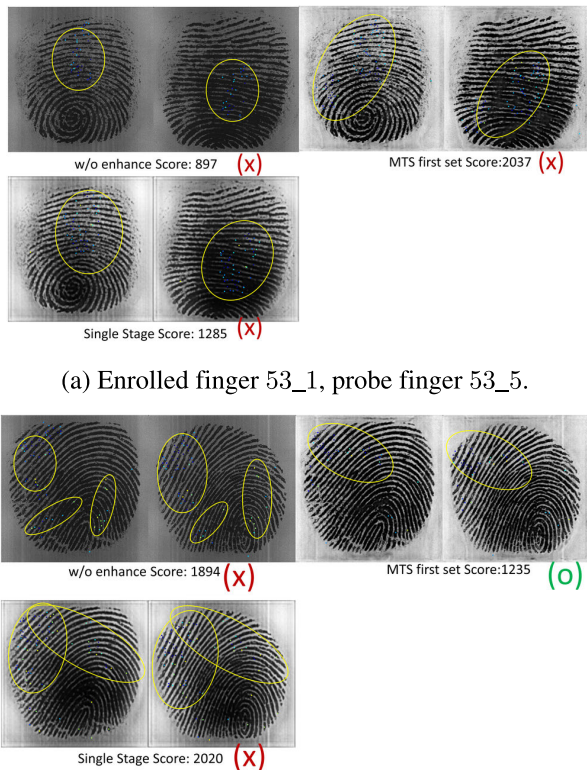
(a) Enrolled finger 53_1, probe finger 53_5.

(b) Enrolled finger 19_3, probe finger 38_1.

FIGURE 15. The effect of imposter score for recognition system.

FIGURE 16. Visualization Results of our proposed method with other approaches. The origin fingerprint is failed to recognition.

first set and single stage approach. We use the FVC protocol to test the results, which are shown in more detail in Table 2. It can be seen that MTS achieved better results than the single stage approach [2]. In Fig.14, it can be seen that if the imposter scores are separated from the genuine scores, the performance of the matching system will improve. Our goal is to lower the imposter scores and raise the genuine scores. In Fig.15 (a), it can be seen that even if the matching score improves, the recognition rate may not be improved if the imposter score is high. In Fig.15 (b), it can be seen that to prevent the imposter score from being too high, improving the exact pattern on the fingerprint is an acceptable alternative that can be accepted by the recognition system. The symbol (o) indicates a correct result, while (x) indicates an incorrect result.

2) EFFECT OF THE MTS AND CCRGAN L_p ON FVC2004 DB4A

This section compares the results of MTS with and without CCRGAN L_p, as well as with single stage on the FVC2004
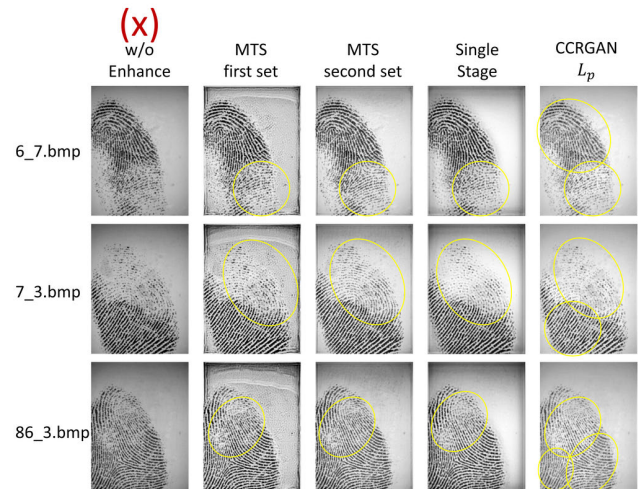
DB4A dataset. The comparison is done using the FVC protocol. The results are presented in Table 3. For MTS without CCRGAN pseudo low L_p, the enrolled number, probe number, genuine count, imposter count, image size, and user number are 300, 500, 500, 79200, 288 × 384, and 100, respectively. With CCRGAN pseudo low L_p, the enrolled number, probe number, genuine count, imposter count, image size, and user number are 600 (300 enhanced + 300 pseudo low), 500, 500, 108900, 288 × 384, and 100, respectively. In the FVC2004 DB4A dataset, the best result is achieved by the MTS second set with CCRGAN L_p. The threshold for each model is taken as the FMR50000 score.

3) COMPARISON WITH STATE-OF-THE-ART RESULTS

We compare the Equal Error Rate (EER) of our proposed method with other methods, as shown in Table 4. In FVC2002 DB1, DB3 and FVC2004 DB3, our method achieved the lowest EER, but have a higher EER than Li et al. [3] in FVC2002 DB4, FVC2004 DB1, DB2, and DB4. Nonetheless, our inference time is about 50 times faster than Li et al. [3], as shown in Table 5. While Li et al. [3] achieved great results through repeated implementation of their method for FVC2004 DB1, DB2, and DB4, our method only needs to be executed once to achieve good results, making our inference time time about 50 times faster than theirs. AS for FVC2002 DB2, our performance is not better than [32], due to the difference in dpi(569) from FVC2000. However, our method outperforms [32] for other datasets

TABLE 4. The quantization result on FVC2002 and FVC2004.

Method	EER(%) FVC2002				EER(%) FVC2004			
	DB1	DB2	DB3	DB4	DB1	DB2	DB3	DB4
[26]	—	—	—	—	3.12	2.50	—	4.19
[27]	2.07	0.88	—	1.53	5.65	5.46	—	2.59
Verifinger	0.25	0.31	—	0.35	1.80	0.82	—	1.06
[2]	0.18	0.14	—	0.25	1.83	3.66	—	0.32
[28]	1.00	0.14	—	0.25	1.83	3.66	—	0.32
[29]	—	—	—	—	7.23(8.46)	—	—	—
[3]	0.25	0.62	—	**0.23**	**1.24**	**0.93**	—	**0.3**
[30]	—	—	—	—	6.39	3.45	1.66	1.33
[1]	0.09	0.23	3.02	—	1.99	3.89	3.90	—
[21]	—	23.95	—	—	—	—	—	—
[31]	0.364	0.538	2.395	—	—	5.925	—	—
[32]	0.23	**0.08**	1.46	—	—	3.25	—	—
MTS first set	**0.02**	0.60	**0.40**	4.80	2.20	3.80	1.80	4.20
MTS first set+L_p	**0.00**	**0.40**	0.42	3.20	1.80	1.63	**1.60**	2.00
MTS second set	**0.05**	0.40	**0.60**	2.00	2.40	2.20	**1.60**	0.60
MTS second set+L_p	**0.04**	2.00	**0.40**	1.46	1.80	2.00	**0.40**	0.40

TABLE 5. Inference time result.

Data-sets/CPU time(s)/Subsets	Method	DB1B	DB2B	DB3B	DB4B
FVC2000	MTS 1st set	4.85	5.09	10.26	4.43
	MTS 2nd set	0.71	0.74	1.48	0.68
	[3]	53.96	40.47	54.90	43.74
FVC2002	MTS 1st set	7.34	8.39	4.93	5.84
	MTS 2nd set	1.06	1.22	0.70	0.84
	[3]	55.41	37.77	58.72	42.42
FVC2004	MTS 1st set	14.54	6.46	7.37	5.96
	MTS 2nd set	2.02	0.87	1.06	0.87
	[3]	53.26	43.37	44.23	45.33

(FVC2002 DB1, DB3, FVC2004 DB2), which are all 500 dpi. In addition, it can be observed that our methods achieve the lowest Equal Error Rate (EER) compared to other methods in the FVC2002 DB1, DB2, and DB3 datasets in Table.4. However, it exhibits a high EER on the DB4 dataset. We observed that most of the fingerprint images in the FVC2002 DB4 dataset have black dots. In addition, texture loss assists in denoising fingerprint images. Therefore, the color of the enhanced fingerprint images becomes lighter. However, template-based matching may consider the ridge colors. This will result in a lower score for FVC2002 DB4. The visualization results of the MTS first set, MTS second set, CCRGAN, and single stage are shown in Fig.16.

VI. CONCLUSION
Our methods achieve the state of the art on FVC2002 DB1 A, FVC2004 DB1A and FVC2004 DB3 A, even though they are only trained on FVC2000. In addition, we have better results than others on the rest of the dataset. This is a challenging task in machine learning, as the trained model is prone to be limited to the domain of the training data. Our method is highly effective for low temperature fingerprints. The MTS models do a great job for enhancing fingerprints, and CCRGAN is more effective in separating the scores between imposter and genuine. In FVC2002 DB1A, the performance of MTS achieve 0.00% on EER with pseudo low templates produced by CCRGAN, which is better than [1] and [2]. In addition, our inference time is 83 times faster than [3] on FVC2002 DB3 B.

REFERENCES
[1] Y. Li, L. Pang, H. Zhao, Z. Cao, E. Liu, and J. Tian, "Indexing-min–max hashing: Relaxing the security–performance tradeoff for cancelable fingerprint templates," *IEEE Trans. Syst., Man, Cybern., Syst.*, vol. 52, no. 10, pp. 6314–6325, Oct. 2022.

[2] W. J. Wong and S.-H. Lai, "Multi-task CNN for restoring corrupted fingerprint images," *Pattern Recognit.*, vol. 101, May 2020, Art. no. 107203.

[3] Y. Li, Q. Xia, C. Lee, S. Kim, and J. Kim, "A robust and efficient fingerprint image restoration method based on a phase-field model," *Pattern Recognit.*, vol. 123, Mar. 2022, Art. no. 108405.

[4] B. G. Sherlock, D. M. Monro, and K. Millard, "Fingerprint enhancement by directional Fourier filtering," in *Proc. Vis. Image Signal Process.*, Apr. 1994, pp. 87–94.

[5] L. Hong, Y. Wan, and A. Jain, "Fingerprint image enhancement: Algorithm and performance evaluation," *IEEE Trans. Pattern Anal. Mach. Intell.*, vol. 20, no. 8, pp. 777–789, Aug. 1998.

[6] Z. Shen, Y. Xu, and G. Lu, "CNN-based high-resolution fingerprint image enhancement for pore detection and matching," in *Proc. IEEE Symp. Ser. Comput. Intell. (SSCI)*, Dec. 2019, pp. 426–432.

[7] J. Li, J. Feng, and C.-C.-J. Kuo, "Deep convolutional neural network for latent fingerprint enhancement," *Signal Process., Image Commun.*, vol. 60, pp. 52–63, Feb. 2018.

[8] S. Adiga and J. Sivaswamy, "FPD-M-net: Fingerprint image denoising and inpainting using M-net based convolutional neural networks," 2018, *arXiv:1812.10191*.

[9] Z. Chen and C. Kuo, "A topology-based matching algorithm for fingerprint authentication," in *Proc. 25th Annu. IEEE Int. Carnahan Conf. Secur. Technol.*, 1991, pp. 84–87.

[10] B. Bhanu and X. Tan, "Fingerprint indexing based on novel features of minutiae triplets," *IEEE Trans. Pattern Anal. Mach. Intell.*, vol. 25, no. 5, pp. 616–622, May 2003.

[11] R. Singh, M. Vatsa, and A. Noore, "Fingerprint indexing using minutiae and pore features," in *Proc. Int. Conf. Image Process., Comput. Vis., Pattern Recognit.*, Jan. 2009, pp. 870–875.

[12] J. Jaam, M.-L. Rebaiaia, and A. Hasnah, "A fingerprint minutiae recognition system based on genetic algorithms," *Int. Arab J. Inf. Technol.*, vol. 3, pp. 242–248, Jan. 2006.

[13] Q. Zhao, L. Zhang, D. Zhang, and N. Luo, "Direct pore matching for fingerprint recognition," in *Advances in Biometrics*, M. Tistarelli and M. S. Nixon, Eds. Berlin, Germany: Springer, 2009, pp. 597–606.

[14] M. A. Medina-Pérez, M. García-Borroto, A. E. Gutierrez-Rodríguez, and L. Altamirano-Robles, "Improving fingerprint verification using minutiae triplets," *Sensors*, vol. 12, no. 3, pp. 3418–3437, Mar. 2012. [Online]. Available: https://www.mdpi.com/1424-8220/12/3/3418

[15] S. A. Sudiro, "Adaptable fingerprint minutiae extraction algorithm based-on crossing number method for hardware implementation using FPGA device," *Int. J. Comput. Sci., Eng. Inf. Technol.*, vol. 2, no. 3, pp. 1–30, Jun. 2012.

[16] C. Ryu, H. Kim, and A. K. Jain, "Template adaptation based fingerprint verification," in *Proc. 18th Int. Conf. Pattern Recognit. (ICPR)*, vol. 4, 2006, pp. 582–585.

[17] R. Cappelli, A. Lumini, D. Maio, and D. Maltoni, "Evaluating minutiae template vulnerability to masquerade attack," in *Proc. IEEE Workshop Autom. Identificat. Adv. Technol.*, Jun. 2007, pp. 174–179.

[18] T. Le and H. Tam, "Fingerprint recognition using standardized fingerprint model," *Int. J. Comput. Sci. Issues*, vol. 7, pp. 1–7, May 2010.

[19] Z. Jin, A. Teoh, T. S. Ong, and T. Connie, "Secure minutiae-based fingerprint templates using random triangle hashing," in *Proc. Int. Vis. Inform. Conf.*, vol. 5857, Nov. 2009, pp. 521–531.

[20] R. Bansal, P. Arora, M. Gaur, P. Sehgal, and P. Bedi, "Fingerprint image enhancement using type-2 fuzzy sets," in *Proc. 6th Int. Conf. Fuzzy Syst. Knowl. Discovery*, vol. 3, 2009, pp. 412–417.

[21] M. Sahasrabudhe and A. Namboodiri, "Fingerprint enhancement using unsupervised hierarchical feature learning," in *Proc. Indian Conf. Comput. Vis. Graph. Image Process.*, Dec. 2014, pp. 1–8.

[22] H. Suzuki, M. Yamaguchi, M. Yachida, N. Ohyama, H. Tashima, and T. Obi, "Experimental evaluation of fingerprint verification system based on double random phase encoding," *Opt. Exp.*, vol. 14, no. 5, pp. 1755–1766, Mar. 2006. [Online]. Available: http://opg.optica.org/oe/abstract.cfm?URI=oe-14-5-1755

[23] L. A. Gatys, A. S. Ecker, and M. Bethge, "Texture synthesis using convolutional neural networks," in *Proc. Adv. Neural Inf. Process. Syst. (NIPS)*, 2015, pp. 1–9.

[24] M. Tuchler, A. C. Singer, and R. Koetter, "Minimum mean squared error equalization using a priori information," *IEEE Trans. Signal Process.*, vol. 50, no. 3, pp. 673–683, Mar. 2002.

[25] J.-Y. Zhu, T. Park, P. Isola, and A. A. Efros, "Unpaired image-to-image translation using cycle-consistent adversarial networks," in *Proc. IEEE Int. Conf. Comput. Vis. (ICCV)*, Oct. 2017, pp. 2242–2251.

[26] J. Yang, N. Xiong, and A. V. Vasilakos, "Two-stage enhancement scheme for low-quality fingerprint images by learning from the images," *IEEE Trans. Hum.-Mach. Syst.*, vol. 43, no. 2, pp. 235–248, Mar. 2013.

[27] P. Sutthiwichaiporn and V. Areekul, "Adaptive boosted spectral filtering for progressive fingerprint enhancement," *Pattern Recognit.*, vol. 46, no. 9, pp. 2465–2486, Sep. 2013.

[28] M. Ferrara, D. Maltoni, and R. Cappelli, "Noninvertible minutia cylinder-code representation," *IEEE Trans. Inf. Forensics Security*, vol. 7, no. 6, pp. 1727–1737, Dec. 2012.

[29] Y. Tu, Z. Yao, J. Xu, Y. Liu, and Z. Zhang, "Fingerprint restoration using cubic Bezier curve," *BMC Bioinf.*, vol. 21, no. S21, pp. 1–19, Dec. 2020.

[30] C. Gottschlich, "Curved-region-based ridge frequency estimation and curved Gabor filters for fingerprint image enhancement," *IEEE Trans. Image Process.*, vol. 21, no. 4, pp. 2220–2227, Apr. 2012.

[31] S. M. Abdullahi, H. Wang, and T. Li, "Fractal coding-based robust and alignment-free fingerprint image hashing," *IEEE Trans. Inf. Forensics Security*, vol. 15, pp. 2587–2601, 2020.

[32] Q. N. Tran and J. Hu, "A multi-filter fingerprint matching framework for cancelable template design," *IEEE Trans. Inf. Forensics Security*, vol. 16, pp. 2926–2940, 2021.
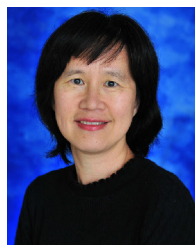
CHING-TE CHIU received the B.S. and M.S. degrees from National Taiwan University, Taipei, Taiwan, and the Ph.D. degree in electrical engineering from the University of Maryland, College Park, MD, USA. She was a member of Technical Staff with AT&T, Lucent Technologies, Murray Hill, NJ, USA, and with Agere Systems, Murray Hill. She is currently a Professor with the Computer Science Department and the Institute of Communications Engineering, National Tsing Hua University, Hsinchu, Taiwan. She is also the Director of the Institute of Information Systems and Applications, National Tsing Hua University. Her research interests include machine learning, pattern recognition, high dynamic range image and video processing, super-resolution, high-speed SerDes design, multi-chip interconnect, and fault tolerance for network-on-chip design. She is a TC Member of the IEEE Circuits and Systems Society, Nanoelectronics and Gigascale Systems Group. She received the First Prize Award, the Best Advisor Award, and the Best Innovation Award of the Golden Silicon Award. She served as the Chair for the IEEE Signal Processing Society, Design and Implementation of Signal Processing Systems (DISPS) TC. She was the Program Chair of the first IEEE Signal Processing Society Summer School, Hsinchu, in 2011, and the Technical Program Chair of the IEEE Workshop on Signal Processing System (SiPS) 2013. She served as an Associate Editor for IEEE TRANSACTIONS ON CIRCUITS AND SYSTEMS—I: REGULAR PAPERS and served as an Associate Editor for *IEEE Signal Processing Magazine* and *Journal of Signal Processing Systems*.

CHIA-YU KUAN received the bachelor's degree from the Department of Computer Science, National Yang Ming Chiao Tung University, and the master's degree from the Department of Computer Science, National Tsing Hua University. She is currently a Camera Image Algorithm Engineer, utilizing her expertise to develop advanced algorithms for image processing. During her studies, she specialized in deep learning and 3D image reconstruction.

YU-CHI SU received the B.S. degree in computer science from National Tsing Hua University, in 2021. She is currently pursuing the M.S. degree with Tsinghua University. During the bachelor's studies, she conducted on cloud computing. In her master's career, she primarily focused on industry-academia collaboration with Novatek Microelectronics Corporation. Her research interests include fingerprint recognition and deep learning.

CHIH-HAN CHENG received the B.S. degree in applied physics from the National University of Kaohsiung, in 2019, and the M.S. degree in computer science from National Tsing Hua University, in 2022. He is currently a CPU Architecture Engineer with Andes Technology. During the master's career, he researched NLP, deep learning, and fingerprint recognition. He has done some projects about gesture classification with the National Science Council and fingerprint recognition with Novatek Microelectronics Corporation.

KUAN-HSIEN LIU received the B.S. degree from National Central University, in 2010, and the M.S. degree from National Cheng Kung University, Taiwan, in 2012. He is currently a Technical Assistant Manager with Novatek Microelectronics Corporation, with a focus on the algorithm development of various fingerprint identification solutions on mobile devices. During the master's career, his research interests included stereo matching, depth estimation, and 3D object reconstruction.

TSUNG-CHAN LEE received the B.S. degree in computer science and information engineering from National Chiao Tung University, Hsinchu, Taiwan, in 2005, and the M.S. degree in computer science from National Tsing Hua University, Hsinchu, in 2007. His study included video surveillance, computer vision, and big data analytics. From 2008 to 2015, he was with Information and Communication Research Laboratories of the Industrial Technology Research Institute. Since 2015, he has been with Novatek Microelectronics Corporation. His research interests include image processing and fingerprint recognition.

WEI-CHANG CHUN received the B.S. degree in mechanical engineering from Yuan Ze University, Taoyuan, Taiwan, in 2011, and the M.S. degree in biomechatronics engineering from National Taiwan University, Taipei, Taiwan, in 2013. He has been an Algorithm Engineer with Novatek Microelectronics Corporation, Hsinchu, since 2020. His research interests include digital image processing and biometric authentication.

JIA-LIN CHEN received the B.S. degree from National Central University and the M.S. degree from National Tsing Hua University. She is currently an Algorithm Engineer with Novatek Microelectronics Corporation. Her research interests include fingerprint recognition, image processing, and machine learning.

YAO-REN CHANG received the B.S. and M.S. degrees from National Taiwan University, in 2014 and 2017, respectively. He is currently an Algorithm Engineer with Novatek Microelectronics Corporation, Taiwan. He mainly focuses on image processing-related topics, such as computer vision, feature extraction, and image enhancement.

JIE-YU LUO received the B.S. and M.S. degrees from the Department of Computer Science, National Ching Hua University, Hsinchu, Taiwan, in 2019 and 2021, respectively. Since 2021, she has been an Algorithm Engineer with Novatek Microelectronics Corporation, Hsinchu. Her research interests include biomedical image processing and biomedical recognition based on machine learning and statistical signal processing. She is also involved in research related to OLED display panels.

KUAN-YING HO (Member, IEEE) received the B.S. degree in electrical engineering from National Chung Hsing University, Taichung, Taiwan, in 2018, and the M.S. degree in biomechatronics engineering from National Taiwan University, Taipei, Taiwan, in 2021. He is currently an Algorithm Engineer with Novatek Microelectronics Corporation, Hsinchu, Taiwan. His current research interests include fingerprint recognition, anti-spoof, and OLED panel voltage drop compensation.

• • •